6th International Symposium on Three-Dimensional Electromagnetics
Berkeley, California, March 28–30, 2017

3D finite-volume time-domain electromagnetic modeling using unstructured grids

Xushan Lu[1], Colin G. Farquharson[1] and Jianhui Li[2]
[1]Memorial University of Newfoundland, Department of Earth Sciences, St. John's, Canada
[2]China University of Geosciences, Institute of Geophysics and Geomatics, Wuhan, China

Summary

We present a finite-volume time-domain method for modeling three-dimensional electromagnetic problems. This method uses an unstructured Delaunay–Voronoï dual mesh which is a generalization of the standard Yee's staggered grids. Both implicit and explicit methods can be derived on this dual mesh. We demonstrate the implicit discretization of the electric field Helmholtz equation with the finite-volume approach and modeling results for models with complex realistic geometry.

Keywords: electromagnetics, forward modeling, finite volume, time domain, unstructured grids

Introduction

Unstructured tetrahedral meshes enable one to generate a geophysical model which is closer to real complex geological models compared to structured meshes (Lelièvre et al., 2012). It has been shown that the unstructured Delaunay-Voronoï dual mesh, which is a generalization of the famous Yee's grid, can be utilized in the finite-volume (FV) discretization of electromagnetic (EM) problems (Jahandari & Farquharson, 2014). Compared with the finite-element (FE) method, which is also capable of using unstructured grids, the FV method is mathematically less sophisticated and easier to implement. In this paper, we extend this FV method from the frequency domain to the time domain.

The utilization of the orthogonal dual mesh enables one to solve the problem with both explicit and implicit discretizations in time, although only the implicit discretization is presented here. The backward Euler method is effective in solving the very stiff EM problems. It is unconditionally stable, thus larger time step sizes can be used. Unfortunately, implicit methods require solving at each time step a linear system of equations which can be very large depending on the model. However, the coefficient matrix remains the same as long as the time step is kept unchanged, therefore the solution time can be significantly reduced with direct solvers by reusing the factorization (Um et al., 2010).

In this paper, we use the FV method for the semi-discretization of the Helmholtz equation for the electric field on a Delaunay-Voronoï dual mesh and the backward Euler method for the full discretization. The direct solver "MUMPS" (Amestoy et al., 2006) is used to solve the linear system at each time step and the so called "adaptive time-step doubling" method (Um et al., 2010) is adopted to accelerate the solution performance. Modeling results with a loop wire source are presented.

Theory

Governing equations

Assuming the magnetic permeability is constant everywhere and also considering the quasi-static approximation, Faraday's law and Ampère's law in the time domain are written as

$$\nabla \times \mathbf{E} + \mu_0 \frac{\partial \mathbf{H}}{\partial t} = 0, \tag{1}$$

$$\nabla \times \mathbf{H} - \sigma \mathbf{E} = \mathbf{J}_s, \tag{2}$$

where $\mathbf{E}(\mathbf{r}, t)$ is the electric field, $\mathbf{H}(\mathbf{r}, t)$ is the magnetic field, μ_0 is the magnetic permeability of free space, σ is the conductivity, and $\mathbf{r}$ and t are position and time, respectively. $\mathbf{J}_s$ is the electric current source and $\mathbf{J}_s = I\hat{\mathbf{u}}(\mathbf{r} - \mathbf{r}_s)$, where I is the amplitude of the source current, $\mathbf{r}_s$ is the position vector of the source, $\hat{\mathbf{u}}$ is the vector of source direction and δ is the Dirac delta function. Taking the curl of equation 1 and substituting equation 2 into the subsequent equation yields

$$\nabla \times \nabla \times \mathbf{E} + \mu_0 \sigma \frac{\partial \mathbf{E}}{\partial t} = -\mu_0 \frac{\partial \mathbf{J}_s}{\partial t}, \tag{3}$$

which is known as the Helmholtz equation for the electric field.

Semi-discretization with the finite-volume method

The unstructured tetrahedral and Voronoï dual mesh (Fig. 1) is used to discretize the computational do-

main, and the spatial discretization of equation 3 is accomplished by discretizing equations 1 and 2 with the FV method. In Fig. 1, the electric field is defined on the tetrahedral edges (black) and the magnetic field is defined on the Voronoï edges (red). The edges of one mesh are orthogonal to the faces of the other mesh. For a detailed description of the finite-volume scheme for the unstructured dual mesh, the reader is referred to Jahandari and Farquharson (2014).

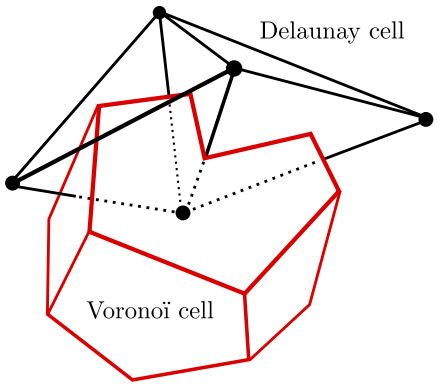

Figure 1: A dual mesh comprised of tetrahedral and Voronoï mesh. The circumcenters of the tetrahedra form the vertices of the Voronoï cells. The edges of the Delaunay (Voronoï) cells are orthogonal to the Voronoï (Delaunay) faces (Jahandari & Farquharson, 2014).

By integrating over the tetrahedral and Voronoï faces and applying Stoke's theorem, equations 1 and 2 become

$$\oint_{\partial A^D} \mathbf{E} \cdot d\mathbf{l}^D = -\mu_0 \iint_{A^D} \frac{\partial \mathbf{H}}{\partial t} \cdot d\mathbf{A}^D, \tag{4}$$

$$\oint_{\partial A^V} \mathbf{H} \cdot d\mathbf{l}^V - \sigma \iint_{A^V} \mathbf{E} \cdot d\mathbf{A}^V = \iint_{A^V} \mathbf{J}_s \cdot d\mathbf{A}^V. \tag{5}$$

In equations 4 and 5, D stands for *Delaunay*, V denotes *Voronoï*, A and ∂A represent the faces and its boundary edges in the dual mesh, $\mathbf{A}$ and $\mathbf{l}$ are unit vectors which are normal to the faces and along the edges, respectively. When considering the electric field along the Delaunay edge and the magnetic field along the Voronoï edge as the respective average of fields over their corresponding orthogonal faces, equations 4 and 5 can be approximated by

$$\frac{dH_j}{dt} = -\frac{1}{\mu_0 A_j^D} \sum_{q=1}^{W_j^D} E_{j,q} l_{j,q}^D, \tag{6}$$

$$\sum_{k=1}^{W_m^V} H_{m,k} l_{m,k}^V - \sigma E_m A_m^V = J_{s_m}. \tag{7}$$

where W denotes the number of edges for the Delaunay or Voronoï faces, m and j represent the global edge index of Voronoï and Delaunay meshes while q and k represent the local edge index of the Delaunay and Voronoï faces corresponding to the jth and mth Voronoï and Delaunay edges.

Taking the derivative of equation 7 with respect to t gives

$$\sum_{k=1}^{W_m^V} l_{m,k}^V \frac{dH_{m,k}}{dt} - \sigma A_m^V \frac{dE_m}{dt} = \frac{dJ_{sm}}{dt}. \tag{8}$$

Finally, the semi-discretization of equation 3 can be obtained by substituting equation 6 into equation 8

$$\frac{dE_m}{dt} = -\frac{dJ_{sm}}{dt} - \sum_{k=1}^{W_m^V} \frac{l_{m,k}^V}{\mu_0 A_{m,k}^D} \sum_{q=1}^{W_{m,k}^D} E_{m,k,q} l_{m,k,q}^D \tag{9}$$

Full discretization

The finite-volume time-domain (FVTD) method is obtained by a full discretization of equation 3, which requires discretizing equation 9 in time. Applying the backward Euler method to equation 9 gives

$$\begin{aligned} &\frac{\Delta t_{n-1}}{\mu_0} \sum_{k=1}^{W_m^V} \frac{l_{m,k}^V}{A_{m,k}^D} \sum_{q=1}^{W_{m,k}^D} E_{m,k,q}^n l_{m,k,q}^D + \sigma E_m^n A_m^V \\ &\quad = \sigma E_m^{n-1} A_m^V - J_{s_m}^n + J_{s_m}^{n-1}, \end{aligned} \tag{10}$$

where n and $n-1$ denote the indices of time instants rather than power. Then the electric field in the time domain can be obtained by solving equation 10 iteratively with proper initial conditions.

Initial and boundary condition

Depending on the type of sources used, the initial condition can be different. For a loop source, there only exists an initial static magnetic field, and the electric field is zero everywhere. Therefore, the right hand side of equation 10 for the first iteration only consists of the change of current density with time since only the electric field is solved. For a galvanic source, there exists a static electric current which involves solving a direct-current resistivity (DCR) problem.

The current density inside the loop wire normally vanishes within a short period of time for realistic instruments. Here, we require the current density to vanish within one iteration, and we call this iteration as the primary iteration. For the second iteration, the amplitude of the current density has already changed from its original value, which is 1 for all the modeling in this paper, to zero and the right-hand side of

equation 10 only consists of the electric field calculated from the primary iteration.

Dirichlet boundary conditions are used for which the electric field on the boundary edges of the Delaunay cells are set to zero for each iteration. The model is set to 50 × 50 × 50 km for all the calculations in order to reasonably approximate these homogeneous conditions of infinity.

Examples

A conductive block in a half-space

First, we present the result of a 3D block embedded in a homogeneous half-space (see Fig. 2), which was first presented by Newman et al. (1986) and has been widely used as a benchmark model. The conductivities of the conductive body, the half-space and the air are 2, 0.1 and $10^{-8}S/m$, respectively. The body is buried 30 m beneath one side of a 100 m by 100 m square loop, with a size of $100 \times 40 \times 30$ m in the $x-$, $y-$ and $z-$directions.

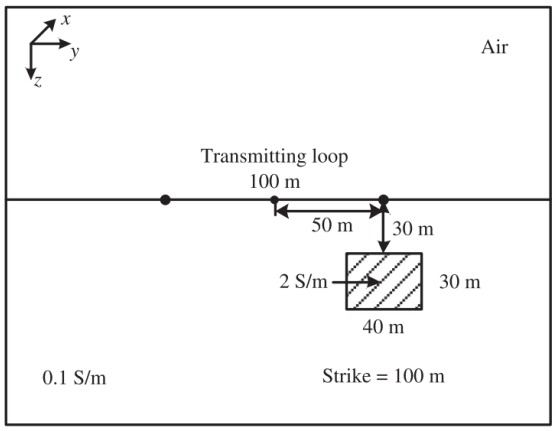

Figure 2: A section view of the 3D block model (Li et al., 2017)

The initial time step is set to 10^{-7} s in this paper for all the calculations. The field response starting from 10^{-7} s to 10^{-2} s is calculated within 790 iterations. Only one observation point is present in the mesh. TetGen (Si, 2015) is used in generating the dual mesh used in this paper. For the block model, the total tetrahedral edge number is 181,815 and the solution time is 293 s on a Linux desktop with a 3.2 GHz quad core processor and 32 GB of RAM.

Fig. 3 shows the numerical results for the 3D block model calculated by different methods together with the analytical and FVTD results of the half-space model within which the 3D block is embedded. For the half-space response, the FVTD result matches the analytical solution very well, with no visible discrepancy observed from the figure. For the block model, the results calculated by the FVTD method and the FE method are close to each other while the FDTD and IE responses are slightly higher and lower, respectively, at the middle times.

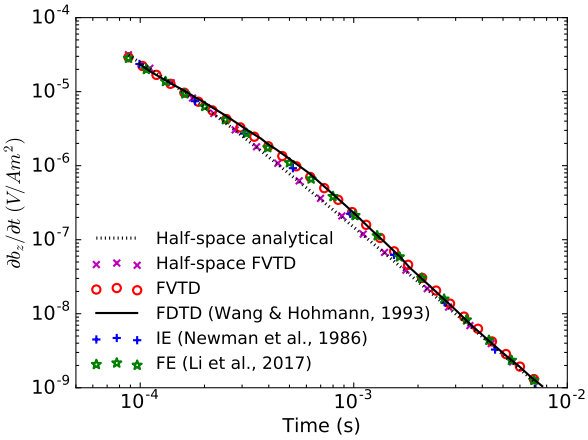

Figure 3: Different numerical results for the block model as calculated by FDTD (Wang & Hohmann, 1993), integral equations (IE) (Newman et al., 1986), the FVTD method presented here, and FE (Li et al., 2017) as well as the analytical and FVTD results of the half-space model.

A massive sulfide deposit with complex geometry

The Ovoid massive sulfide ore body, located at Voisey's Bay, Labrador, Canada, is a well recovered model based on substantial drill data. It is flat lying, composed of 70% massive sulfide and is located approximately 20 m beneath overburden.

Jahandari and Farquharson (2014) presented their modeling results of a helicopter-borne frequency-domain EM survey and compared it with the real data. Li et al. (2017) used the same surface tessellation of the ore body and calculated the time-domain response of the body with a fixed-loop source configuration. Here, we compare the time-domain response calculated by the FVTD method with their results calculated by a FE frequency-to-time transformation.

As shown in Fig. 4, the loop is 500 × 500 m which is located at the elevation of 110 m. The conductivity of the ore body and background half-space model are 100 and 0.001 S/m, respectively. The field response from 10^{-7} s to 0.0329 ms is calculated with 763 iterations. The number of the tetrahedral edges generated by TetGen for this model is 1,498,799, and the solution time of FVTD is 2 hours and 22 minutes.

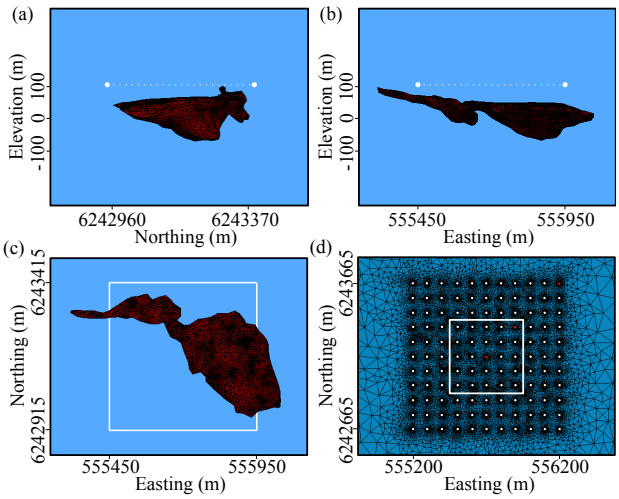

Figure 4: The mesh for the Ovoid Zone model.The white rectangle represents the loop wire. The white and red dots both inside and outside the loop wire are the locations of the observation points (Li et al., 2017).

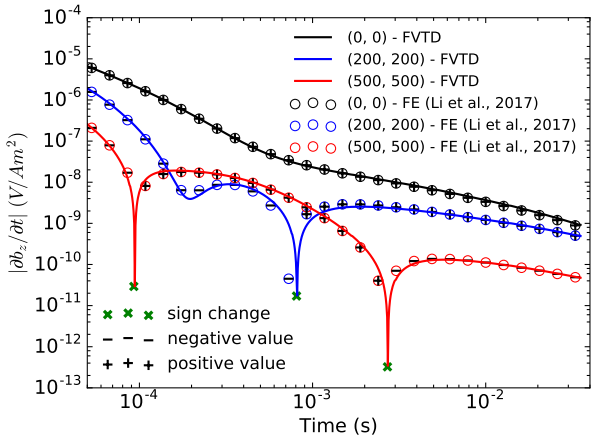

Figure 5: Numerical results of FVTD and FE methods for the same Ovoid Zone model. The observation locations (0, 0), (200, 200) and (500, 500) m are shown in Fig. 4 (the red points), which are relative to the loop center.

The numerical results calculated from FVTD (solid lines) and FE (circles) are shown in Fig. 5. The results at (0, 0) m match very well between the two methods except the late times. For observation points (200, 200) m and (500, 500) m, both results exhibit the sign change phenomenon. Because only the responses of certain time channels are transformed from the frequency domain in the FE method, it cannot depict the rapid field change around the time when the sign is changed. On the other hand, since the time step used in FVTD is normally very small in order to capture the fast decaying EM field, it can easily catch the local minima in the absolute field value graph.

Conclusion

The FV method using unstructured Delaunay-Voronoï dual mesh for calculating frequency-domain EM responses can be readily extended to solving time-domain EM problems as shown here. Numerical tests show that the method has comparable accuracy to FE methods and is capable of modeling time-domain EM responses of ore bodies with complex geometry.

REFERENCES

Amestoy, P. R., Guermouche, A., L'Excellent, J.-Y., & Pralet, S. (2006). Hybrid scheduling for the parallel solution of linear systems. *Parallel Computing*, *32*(2), 136-156.

Haber, E., Ascher, U. M., & Oldenburg, D. W. (2004). Inversion of 3D electromagnetic data in frequency and time domain using an inexact all-at-once approach. *Geophysics*, *69*(5), 1216–1228.

Jahandari, H., & Farquharson, C. G. (2014). A finite-volume solution to the geophysical electromagnetic forward problem using unstructured grids. *Geophysics*, *79*(6), E287–E302.

Lelièvre, P. G., Carter-McAuslan, A., Farquharson, C., & Hurich, C. (2012). Unified geophysical and geological 3D Earth models. *The Leading Edge*, *31*(3), 322–328.

Li, J., Farquharson, C. G., & Hu, X. (2017). 3D vector finite-element electromagnetic forward modeling for large loop sources using a total-field algorithm and unstructured tetrahedral grids. *Geophysics*, *82*(1), E1–E16.

Newman, G. A., Hohmann, G. W., & Anderson, W. L. (1986). Transient electromagnetic response of a three-dimensional body in a layered earth. *Geophysics*, *51*(8), 1608–1627.

Si, H. (2015). Tetgen, a delaunay-based quality tetrahedral mesh generator. *ACM Trans. Math. Softw.*, *41*(2), 11:1–11:36.

Um, E. S., Harris, J. M., & Alumbaugh, D. L. (2010). 3D time-domain simulation of electromagnetic diffusion phenomena: A finite-element electric-field approach. *Geophysics*, *75*(4), F115–F126.

Wang, T., & Hohmann, G. (1993). A finite-difference, time-domain solution for three-dimensional electromagnetic modeling. *Geophysics*, *58*(6), 797–809.